Available online at www.sciencedirect.com
SCIENCE DIRECT
Inorganica Chimica Acta 359 (2006) 1200–1206
Inorganica Chimica Acta
www.elsevier.com/locate/ica

Crystal structure and DNA-binding studies of a new Cu(II) complex involving benzimidazole

Qinghua Zhou, Pin Yang *

Institute of Molecular Science, Chemical Biology and Molecular Engineering, Laboratory of Education Ministry, Shanxi University, Taiyuan 030006, P.R. China

Received 4 August 2005; received in revised form 4 November 2005; accepted 7 November 2005
Available online 27 December 2005

Abstract

A new Cu(II) complex of $CuL(ClO_4)_2$ (here, L = *N*,*N*,*N*′,*N*′-tetrakis[(2-benzimidazolyl)methyl]-1,3-diaminopropane) has been synthesized and characterized by elemental analyses, UV–Vis, FT-IR, cyclic voltammogram and X-ray single crystal diffraction. The Cu(II) environmental in complex is distorted octahedral. π–π stacking interactions stabilize the crystal packing together with the hydrogen-bonding interactions. The interaction of the complex with DNA has been investigated using equilibrium dialysis, UV spectra, fluorescent spectra, and gel electrophoresis. The results show that the Cu(II) complex can electrostatically bind to the phosphate group of DNA backbone, and partially intercalate into the double helix of DNA because of the bulky structure of the complex and the planarity of the benzimidazole rings.

Keywords: Benzimidazole; Cu(II) complex; Calf thymus DNA

1. Introduction

The interaction of small molecules with DNA has been an active area of research at the interface of chemistry and biology [1–6]. These small molecules are stabilized in binding to DNA through a series of weak interactions, such as the π-stacking interactions associated with intercalation of a planar aromatic group between the base pairs, hydrogen-bonding and van der Waals interactions of functionalities bound along the groove of the DNA helix [7], and the electrostatic interaction of the cation with phosphate group of DNA [8]. Studies directed toward the design of site- and conformation-specific reagents provide rationales for new drug design as well as a means to develop sensitive chemical probes of nucleic acid structure. Benzimidazole ring functions as ligand toward transition metal ions in a variety of biologically important molecules [9]. The presence of a rigid aromatic system in the benzimidazole structure gives rise to particular spectroscopic, which make it a potential probes for nucleic acids. Crystallographic [10–12] and NMR studies [13–15] show ligands incorporating benzimidazole can selectively interact with a specific nucleotide sequence, which bind to the minor groove of A–T tract duplex DNA and the benzimidazole unit is a conformationally stable and appropriate platform on which to build further DNA sequence recognition. Metal complexes involving benzimidazole are an important class of biologically active compounds that can efficiently hydrolyze phosphonate diester [16] and cleave the supercoiled pBR322 DNA [17–19].

In this paper, we report the synthesis of the ligand [20,21] that contains four benzimidazole groups and the crystal structure of $CuL(ClO)_2$ (here, L = *N*,*N*,*N*′,*N*′-tetrakis[(2-benzimidazolyl)methyl]-1,3-diaminopropane). The interaction of the complex with DNA has been investigated using equilibrium dialysis,UV spectra, fluorescent spectra and gel electrophoresis.

* Corresponding author. Tel./fax: +86 351 7011022.
E-mail address: yangpin@sxu.edu.cn (P. Yang).

0020-1693/$ - see front matter © 2005 Elsevier B.V. All rights reserved.
doi:10.1016/j.ica.2005.11.003

2. Experimental

2.1. Materials and instruments

Elemental analysis was performed on a Perkin–Elmer 240C instrument, ^{1}H NMR and ^{13}C NMR spectra were obtained on a Bruker DRX-300 spectrometer, absorbance spectra were recorded on a Hewlett–Packard HP-8453 Chemstation spectrometer, fluorescence measurements were made with a Perkin–Elmer LS-50B fluorescence spectrophotometer. IR spectra were recorded on a Shimadzu FT-IR-8300 spectrometer with KBr as discs. Cyclic voltammetry was carried out on a CHI660B electrochemical workstation (CH Instruments, Shanghai, China) connected with a three-electrode cell at room temperature. A glass carbon (GC) working (3 mm in diameter) and a Pt wire counter electrode were employed. The reference electrode is Ag/AgCl (saturated). Solution was prepared by dissolving the complex in DMF, using 0.1mol L^{-1} $NaClO_4$ as supporting electrolyte. Plasmid DNA products were analyzed with a UVP GDS8000 complete gel documentation and analysis system. Calf thymus DNA was obtained from Sigma, UV–Vis spectrometer was employed to check DNA purity (A_{260}:$A_{280} > 1.80$) and concentration ($\varepsilon = 6600$ L mol^{-1} cm^{-1} at 260 nm). All the measurements about interaction of the complex with CT DNA were conducted using solutions of the complex in Tris–HCl buffer (pH 7.5) containing 10 mmol L^{-1} Tris and 5 mmol L^{-1} NaCl. All other reagents were obtained commercially and used without further purification.

2.2. Synthesis

6.13 g (20 mmol) of 1,3-Diaminopropane-*N*,*N*,*N*′,*N*′-tetraacetic acid was combined with 8.65 g (80 mmol) of *o*-phenylenediamine in 50 mL of glycol. The solution was refluxed for 24 h. The resulting yellow solution was poured into 200 mL of water. The white precipitate was collected, recrystallised from hot methanol and dried in vacuo. *Anal*. Calc. for $C_{35}H_{34}N_{10} \cdot 2CH_3OH \cdot 2H_2O$: C, 63.98; N, 20.17; H, 6.63. Found: C, 63.91; N, 20.16; H, 6.70%. UV–Vis spectrum in ethanol λ_{max}/nm (ε_m/L cm^{-1} mol^{-1}): 276 (36 000), 282 (35 740). IR (KBr, cm^{-1}): 2920 (br, s), 1620 (m), 1439 (s), 1272 (s), 740 (s). ^{1}H NMR (DMSO-d_6): 7.49–7.52 (m, 8H), 7.13–7.16 (m, 8H), 3.97 (s, 8H), 2.61 (s, 4H), 1.83 (m, 2H). ^{13}C NMR (DMSO-d_6): 24.09, 51.93, 52.08, 115.24, 121.98, 138.96, 152.92.

To a solution of 0.139 g L (0.2 mmol) in methanol (10 mL), was added dropwise a methanol solution (5 mL) of 0.074 g $Cu(ClO_4)_2 \cdot 6H_2O$ (0.2 mmol). The resulting solution was stirred at room temperature overnight, and filtered. The filtrate were kept at room temperature and the green crystals were crystallized from the solution after 1 week, by slowly evaporating the solvent. *Anal*. Calc. for $C_{35}H_{34}N_{10}Cu\ (ClO_4)_2$: C, 49.04; N, 16.33; H, 3.97. Found: C, 49.25; N, 16.18; H, 3.72%. UV–Vis spectrum in ethanol λ_{max}/nm (ε_m/L cm^{-1} mol^{-1}): 273 (21 840), 279 (21 600). IR (KBr, cm^{-1}): 3050 (br, s), 1624 (m), 1454 (s), 1276 (s), 1118 (s), 1029 (s), 925 (m), 748 (s), 625 (s).

2.3. X-ray crystallographic studies

The raw data of complex was obtained on a Bruker SMART APEX CCD automatic diffractometer. Reflection data were collected at 203 K using Mo Kα radiation ($\lambda = 0.71073$ Å). The collected data were reduced using the program SAINT [22] and empirical absorption correction was carried out using SADABS [23] program. The structure was solved by Patterson methods (SHELXS97) [24] and then refined on F^2 by a full-matrix least-squares procedure using anisotropic displacement parameters [25]. H atoms attached to C atoms were placed in geometrically idealized positions, with $Csp^3 = 0.97$ Å and $Csp^2 = 0.93$ Å, and constrained to ride on their parent atoms, with $U_{iso}(H) = 1.2U_{eq}(C)$. H atoms on N atoms were located in a difference Fourier map and isotropically refined. Atomic scattering factors are from International Tables for X-ray crystallography [26] and molecular graphics from SHELXTL [27]. A summary of the crystal data, experimental details, and refinement results is given in Table 1.

2.4. $[CuL]^{2+}$–DNA interaction studies

A 1 mL sample of calf thymus DNA (0.6 mmol L^{-1}) was dialyzed against 10 mL of buffer plus varying amounts of added complex. These solutions were dialyzed for 3 days

Table 1
Crystal data and structure refinement for complex

Empirical formula	$C_{35}H_{34}Cl_2N_{10}O_8Cu$
Formula weight	857.17
Temperature (K)	203(2)
Crystal system	monoclinic
Space group	*C*2/*c*
a (Å)	17.360 (3)
b (Å)	10.733(2)
c (Å)	19.209 (3)
α (°)	90
β (°)	94.971 (2)
γ (°)	90
V (Å^3)	3565.5 (10)
Z	4
D_{calc} (g cm^{-3})	1.597
Crystal size (mm)	0.40 × 0.30 × 0.30
F(000)	1764
Reflections collected	7280
Unique reflections	3130
θ Range for data collection (°)	2.23–26.58
Index ranges	$-20 \leqslant h \leqslant 15$, $-12 \leqslant k \leqslant 12$, $-20 \leqslant l \leqslant 22$
Absorption coefficient (mm^{-1})	0.832
Data/restrains/parameters	3130/6/262
Final *R* indices [$I > 2\sigma(I)$]	$R_1 = 0.0439$, $R_{w2} = 0.1092$
R indices (all data)	$R_1 = 0.0494$, $R_{w2} = 0.1121$
Goodness-of-fit	1.081
Largest difference in peak and hole (e Å^{-3})	0.441 and −0.284

with continuous agitation on a shaker bath at 30 °C. Free complex concentrations were determined from the dialysate by absorbance measurements at 279 nm ($\varepsilon = 17164$ L cm^{-1} mol^{-1}).

The Cu(II) complex was dissolved in DMSO at a concentration of 0.002 mol L^{-1}. The absorption titrations were performed by keeping the concentration of CT DNA (7.8×10^{-5} mol L^{-1}) constant while varying the complex concentration ($0–1 \times 10^{-5}$ mol L^{-1}). The absorption was recorded after each addition of the complex. It has been verified that the low DMSO percentage added to the DNA solution would not interfere with the nucleic acid [28]. The fluorescent spectra ($\lambda_{ex} = 520$ nm) were also recorded at room temperature. All solutions were allowed to equilibrate thermally for about 30 min before measurements were made.

The interaction of pBR322 DNA by Cu(II) complex was carried out with 10 μL reaction mixture containing of 10 mmol L^{-1} Tris–HCl (pH 7.5 containing 5 mmol L^{-1} NaCl) buffer, varying concentrations of complex, 0.5 μL of pBR322 (0.5 μg/μL) and DMSO fixed to 1 μL. After mixing, the DNA solutions were incubated at 37 °C for 4 h. The reactions were quenched by the addition of EDTA and bromphenol blue. The gel was stained with EB (ethidium bromide) for 0.5 h after electrophoresis, and then photographed.

3. Results and discussion

3.1. The characterization of Cu(II) complex

The crystal of the complex is built of $[CuL]^{2+}$ cations and perchlorate anions. A crystallographic twofold rotation axis passes through the C18 and Cu(II). The structure of the cation is depicted in Fig. 1. The selected geometric parameters are listed in Table 2.

In the molecular structure of the cation, the copper (II) ion lies in a highly distorted octahedral geometry, in which the two bis(2-benzimidazolylmethyl)amine moieties of the ligand are coordinated to two faces of the octahedron. The angles between the two atoms in trans position about Cu(II) are 164.94(9)° and 155.69(8)°, a deviation of nearly 25° from the ideal bond angle of 180°. The idealized 90° octahedral bond angles vary from 76.39(8)° to 127.74(9)°. The benzimidazole rings are nearly planar, the mean deviation from plane 0.038 and 0.017 Å, respectively. The dihedral angles between plane 2 (C8–C14, N2, N5), plane 4 (C8A–C14A, N2A, N5A) and the adjacent planes, viz., plane 1 (C1–C7, N3, N4) and plane 3 (C1A–C7A, N3A, N4A), are 97.3° and 72.8°, respectively. The Cu–$N_{imidazole}$ bond lengths (1.970(2) and 2.090(2) Å, respectively) are shorter than the Cu–N_{amino} bonds (2.459(2) Å), in agreement with values reported previously [29]. This highly distorted geometry is probably a consequence of the geometrical requirements of the chelating ligand. In contrast to the geometric parameters of the ligand and copper(II) in the 1:2 chelate [20], the Cu–N bond lengths and N–Cu–N bond angles vary considerably. The Cu–$N_{imidazole}$ bond lengths (1.970(2) and 2.090(2) Å, respectively) in the 1:1 complex are somewhat longer than those of the 1:2 complex (1.953(7) and 1.955(7) Å, respectively), whereas, the Cu–N_{amino} bond

Table 2
Selected bond lengths (Å), angles (°) and torsion angles (°)

Cu–N1	2.459 (2)
Cu–N2	1.970 (2)
Cu–N3	2.090 (2)
N1–Cu–N2	90.37 (9)
N1–Cu–N3	76.39 (8)
N1–Cu–N1A	79.74 (8)
N1–Cu–N2A	78.02 (9)
N1–Cu–N3A	155.69 (8)
N2–Cu–N3	97.53 (9)
N2–Cu–N2A	164.94 (9)
N2–Cu–N3A	89.11 (9)
N3–Cu–N3A	127.74 (9)

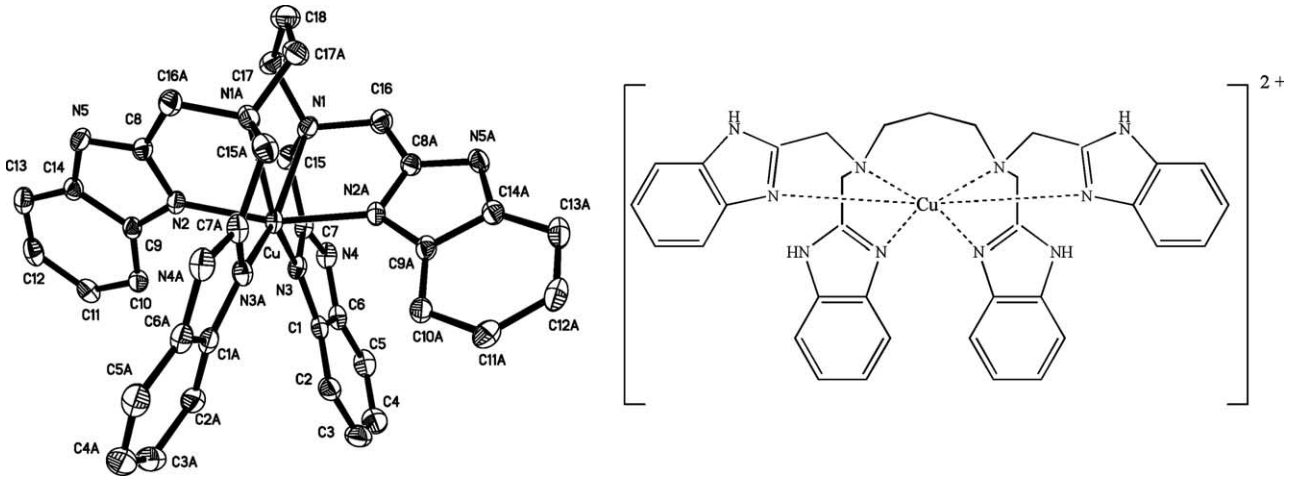

Fig. 1. The structure of $[CuL]^{2+}$ in 30% probability ellipsoids (left) and the scheme of $[CuL]^{2+}$ (right). H atoms and counter-ions have been omitted for clarity. [Symmetry code: A $-x$, y, $0.5 - z$].

distance (2.459(2) Å) obviously increases about 0.35 Å as compared with that of the 1:2 complex (2.102(7) Å). The $N_{imidazole}$–Cu–N_{amino} bond angles are 90.37(9) and 76.39(8)° in the 1:1 complex, and 80.9(3) and 81.9(3)° in the 1:2 complex, respectively. The large difference between the two complexes is that $N_{imidazole}$–Cu–$N_{imidazole}$ bond angle in the 1:1 complex (89.11(9) °C) is 72.4 °C less than that of 1:2 complex (161.5(3)°). The above differences are presumably a consequence of the stereochemical requirements of the ligand in the different coordination mode.

The pyrrole nitrogens N5, N4 of the benzimidazole rings are involved in hydrogen bonding, the former with O1 and the latter with O2 of ClO_4^-[$N5\cdots O1(-x,1-y,-z) = 2.784(4)$ Å, $N4\cdots O2(1/2-x, -1/2+y, 1/2-z) = 2.883(4)$ Å], respectively. Neighboring benzimidazole rings (plane 2 which contains C14 and 5 which contains $C14(-x,-y,-z)$), are parallel in an offset fashion and separated by a face-to-face distance of 3.496 (4) Å. This fact indicates the existence of π–π stacking interactions, which stabilize the crystal packing together with the hydrogen-bonding interactions.

Compared to the spectrum of the free ligand, Two absorption bands at 276 and 282 nm ascribed to the intra-ligand π–π* transitions of the benzimidazolyl groups, is blue-shifted coordination (273 and 279 nm, respectively), showing C=N coordination to copper center [29]. In the IR, the 1620 cm^{-1} band attributed to $\nu_{C=N}$ stretching and 1439 cm^{-1} band assigned to $\nu_{s(-C=N-C=C-)}$ of the free ligand, are considerably shifted towards lower frequencies (1624 and 1454 cm^{-1}, respectively), implying direct coordination of the benzimidazolyl nitrogens to copper(II) [30]. These results agree with those of the single-crystal X-ray diffraction study.

Fig. 2 depicts the electrochemical property of the CuL complex in DMF solution containing 0.1 mol L^{-1} $NaClO_4$ at scan rate 20 mV/s. The CV diagram of complex shows a pair of redox peaks with $E_{pa} = -0.206$ V ($i_{pa} = -1.24 \times 10^{-7}$A) and $E_{pc} = -0.357$ V ($i_{pc} = 2.04 \times 10^{-7}$ Å). The couple was quasi–reversible one-electron redox with $\Delta E = 0.151$ V and $i_{pa}/i_{pc} = 0.6$ (i_{pa} and i_{pc} are the anodic and cathodic currents, respectively) corresponding to the Cu(II)/Cu(I). The ΔE and i_{pa}/i_{pc} values imply that there is some irreversibility to the electron transfer reaction, which suggests that a coordination change takes place at the copper ion upon oxidation or reduction on the electrochemical time scale [31].

3.2. Equilibrium dialysis

The binding constant of complex binding to DNA may be determined by classical dialysis experiment. Data of Fig. 3 were obtained by equilibrium dialysis and performed by nonlinear least-squares fitting of the data of Fig. 3 to McGhee–von Hippel equation [7]. The binding constant obtained for CuL($1.21(\pm 0.14) \times 10^4$ L mol^{-1}) is 2–3 orders of magnitude lower than those measured for the proven intercalators ethidium (2.5×10^6 L mol^{-1}) and daunomycin (2.5×10^7 L mol^{-1}) [8] (extrapolated to the ionic strength of our buffer), implying that interaction of CuL to DNA may be essentially electrostatic binding or partial insertion [32]. It is understandable from the structure of the complex. The octahedral coordination around the Cu(II) precludes effective stacking of the complex between base pairs. When one of the four benzimidazole rings inserts into the helix, the adjacent two benzimidazole rings actually protrude above and below the face of the planes and decrease the effective area of overlap due to the stereochemistry effect. Hence, a single benzimidazole ring cannot completely intercalate because of the bulky structure of CuL. Partial intercalation may occur. The small region of overlap with only partial insertion is necessary for a stabilizing interaction with the duplex [32]. Concomitantly, the hydrogens of pyrrole N atoms in the benzimidazole rings may favor their hydrogen bonding to DNA [33] and thus stabilize the complex bound to DNA.

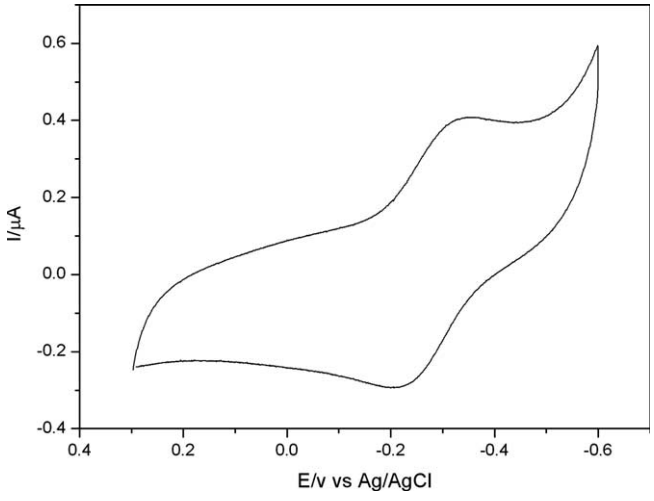

Fig. 2. Cyclic voltammogram of CuL (1×10^{-4}mol L^{-1}) in DMF solution.

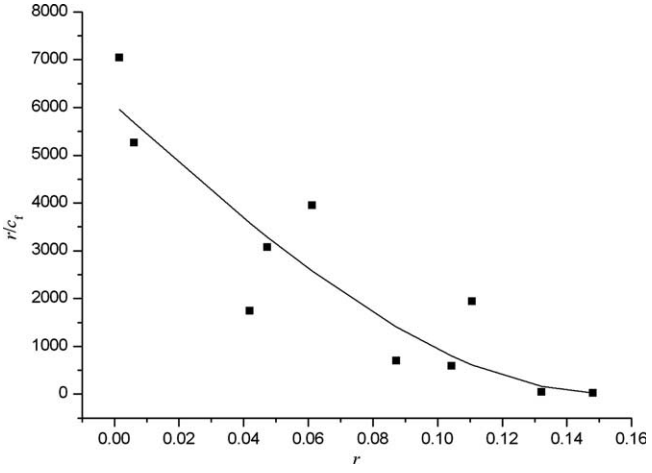

Fig. 3. Scatchard plot of the binding of CuL with calf thymus DNA in buffer at 30 °C, where r is the ratio of bound CuL to total nucleotide concentration, C_f is the concentration of free CuL.

3.3. UV spectroscopic studies

"Hyperchromic effect" and "hypochromic effect" are the spectra features of DNA concerning its double-helix structure [34]. Fig. 4 shows the absorption spectra of DNA alone in the presence of CuL with various concentrations (with subtraction of CuL absorbance). The absorption decreased significantly upon addition of complex, indicating interaction of the complex with DNA. CuL^{2+} can make a contraction in the helix axis of DNA by electrostatic binding to the phosphate group of DNA backbone. Concomitantly, partial intercalation act as a "wedge" to pry apart one side of a base pair stack but not fully separate the stack as required by the classical intercalation model [8]. The possible result is a static bend or kink in the helix, which results in a reduction in helix end-to-end distance. Those cause the hypochromism of DNA [34].

3.4. Fluorescence spectroscopic studies

3.4.1. Effect of complex on the fluorescence spectra of DNA–EB complex

In order to investigate the mode of the Cu(II) complex binding to DNA, the competitive binding experiment has carried out. The fluorescent emission of EB (2 μmol L^{-1}) bound to DNA (20 μmol L^{-1}) in the absence and the presence of complex is shown in Fig. 5. EB is a conjugate planar molecule. Its fluorescence intensity is very weak, but it is greatly increased when EB is specifically intercalated into the base pairs of double-stranded. When EB is free from DNA, the fluorescence of DNA–EB complex is quenched evidently. Therefore, EB can be used as a probe for DNA structure detection [35]. CuL does not itself show appreciable fluorescence in the spectral region studied, either free or bound to DNA, and does not quench the fluorescence of EB in the absence of DNA under the conditions of our experiments (as shown in Fig. 6). The emission band at 600 nm of the DNA–EB system decreased in intensity on increasing the Cu(II) complex concentration. When the complex was added to 1×10^{-5} mol L^{-1} ($R_t = C_{CuL}/C_{DNA} = 0.5$), the fluorescence intensity did not obviously decrease any more. It may be due to the binding of the cationic CuL^{2+} to the negatively charged oxygen of phosphodiester of DNA, and it causes a contraction of DNA which drives a few EB molecules out of DNA.

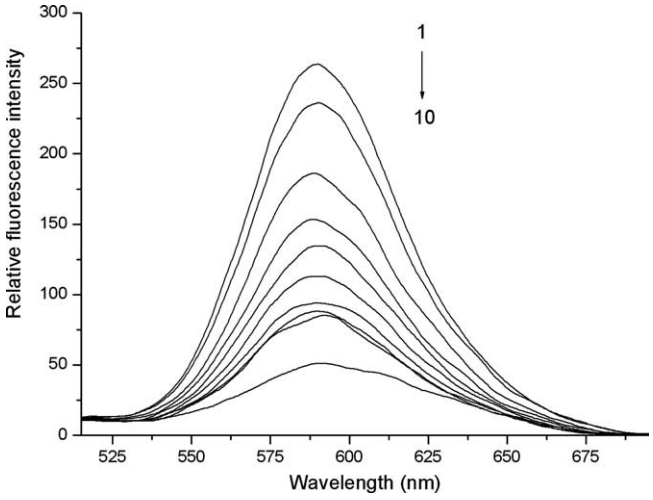

Fig. 5. Fluorescence emission spectra (excited at 520 nm) of EB(10), EB–DNA complexes in the absence (1) and presence (2–9) of increasing concentrations of the complex (2 mmol L^{-1}, 1 μL per scan).

3.4.2. Scatchard plots

To get a better insight into the nature of complex-DNA binding, we have carried out a fluorescence study of EB to DNA in the presence of a competing metal complex. The characteristics of the binding of EB to DNA can be expressed by Scatchard equation [35].

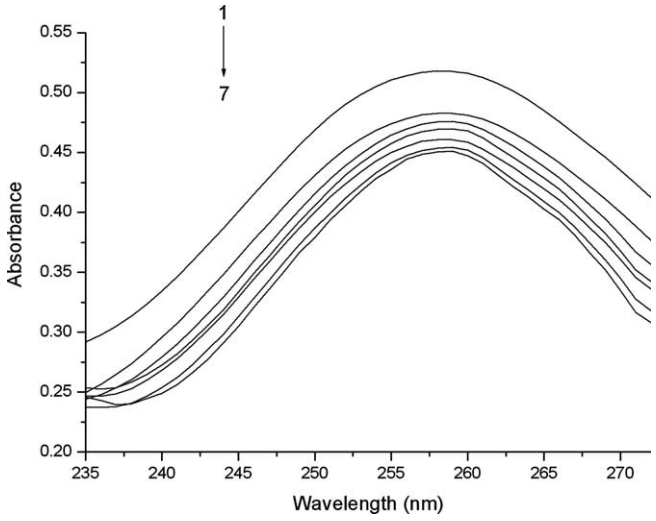

Fig. 4. Absorption spectra of calf thymus DNA (1, 7.8×10^{-5}mol L^{-1}) in Tris–HCl buffer upon addition of CuL (2–7, 1, 4, 6, 8, 9, 10×10^{-6} mol L^{-1}, respectively.).

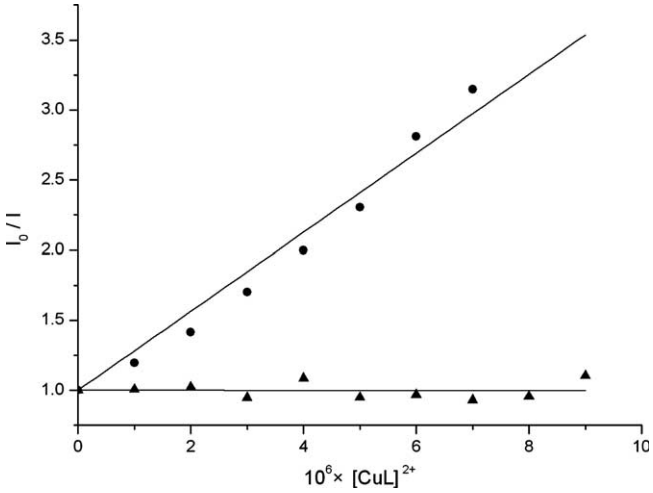

Fig. 6. Fluorescence quenching of CuL to EB–DNA complex (●) and EB (▲).

$r/C_f = K(n - r)$.

Here, r is the ratio of bound EB to total nucleotide concentration, C_f is the concentration of free EB, n is the number of binding sites per nucleic acid, K is the intrinsic binding constant for EB. Fluorescence Scatchard plots for the binding of EB to CT DNA (2.0×10^{-5} mol L^{-1}) in the presence of CuL (5×10^{-6} mol L^{-1}) are given in Fig. 7. Both the K and n change, which indicates that the complex binds to DNA by a mixed mode, namely, by both uncompetitive and competitive inhibitions [36]. The uncompetitive inhibition is due to the binding of the CuL^{2+} to DNA via the phosphate group. The competitive inhibition is probably due to partial insertion of the planar benzimidazole ring into DNA, blocking potential intercalation sites of EB and competing for the intercalative binding sites with EB.

3.4.3. Mechanism for the fluorescence quenching

In order to investigate the effect of temperature, the fluorescence intensity of DNA–EB complex with various concentrations of CuL was measured at different temperature. The fluorescence quenching data follows the Stern–Volmer equation:

$I_0/I = 1 + K[Q]$,

where I_0 and I are the fluorescence intensities from the excited DNA–EB in both the absence and the presence of the given copper(II) complex concentrations, respectively, $[Q]$ is the concentration of the Cu(II) complex. As shown in Fig. 8, in the presence of 2.0×10^{-5} mol L^{-1} DNA and 2.0×10^{-6} mol L^{-1} EB, from 0 to 9.0×10^{-6} mol L^{-1} CuL, the plots of I_0/I versus $[Q]$ are linear, as expected from the Stern–Volmer quenching equation. Since the dynamic quenching is due to the diffusion, the slope (K) should be increased with increasing temperature. On the contrary, increasing temperature will make the stability of the CuL–EB–DNA compound decrease, therefore, K in static quenching process should be decreased with the increasing temperature. As it is expected for a static quenching, our experimental observation indicates that its efficiency diminishes as the temperature increases. This fact suggests that the quenching observed in steady state experiments is mainly static [37].

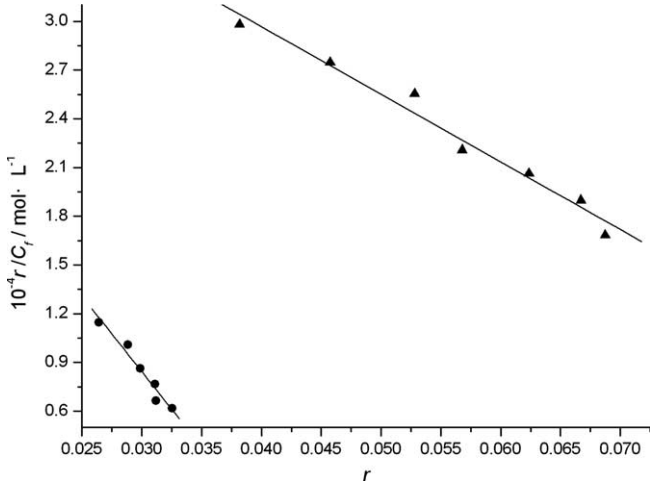

Fig. 7. Fluorescence Scatchard plots of the binding of EB to CT DNA in the absence (▲) and the presence (●) of the complex (5×10^{-6} mol L^{-1}).

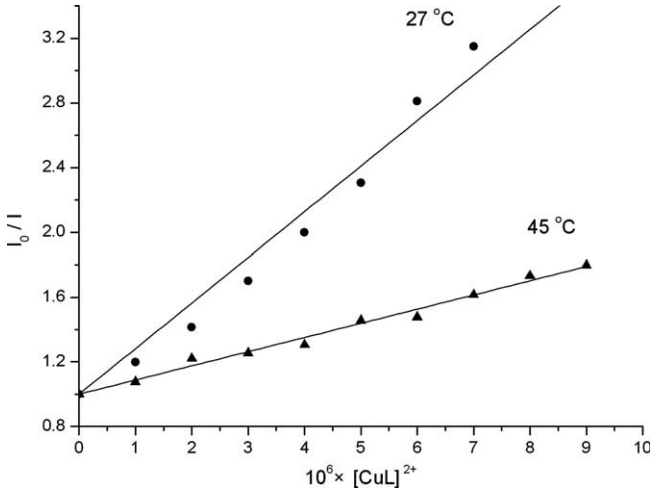

Fig. 8. Fluorescence quenching of CuL to EB–DNA system at different temperature.

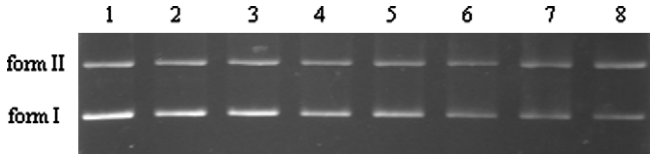

Fig. 9. Electrophoretic analysis of pBR322 DNA (72 μmol L^{-1} (p)) mixed with various concentrations of the complex. Lane 1: DNA control; Lanes 2–8: 0.1, 0.5, 1, 2, 3, 5, 10×10^{-5} mol L^{-1} the Cu(II) complex, respectively.

3.5. Electrophoretic analysis

Further insight into the interaction between the Cu(II) complex and DNA was obtained using gel electrophoresis. As shown in Fig. 9, no evidence was found for DNA cleavage by the complex. The fluorescence became gradually weak with the increase of the concentration of the Cu(II) complex. It maybe due to the extensive binding of CuL^{2+} into double helix of DNA, and there are few binding sites on DNA for EB. When $R_t > 0.5$, the fluorescence intensity didn't obviously change. The data show the decreased emission from EB in lanes 2–8 indicative of the same phenomena that gave rise to this reduced emission in Fig. 5.

4. Conclusions

In summary, a new Cu(II) complex, $CuL(ClO_4)_2$, has been synthesized and characterized by elemental analyses, UV–Vis, FT-IR, cyclic voltammogram and X-ray single crystal diffraction. Equilibrium dialysis, UV spectra, fluorescent spectra, and gel electrophoresis studies suggest that the complex can electrostatically bind to the phosphate

group of DNA backbone and partially intercalate into the double helix of DNA because of the bulky structure of the complex and the planarity of the benzimidazole rings. Further studies will be performed in order to fully clarify the mode of the interaction.

5. Supplementary material

CCDC 278361 contains the supplementary crystallographic data for this paper. These data can be obtained free of charge via www.ccdc.cam.ac.uk/data_request/cif, or by e-mailing data_request@ccdc.cam.ac.uk, or by contacting The Cambridge Crystallographic Data Centre, 12, Union Road, Cambridge CB2 1EZ, UK; fax: +44 1223 336033.

Acknowledgements

We are grateful for financial support of the National Natural Science Foundation of China (grant No. 30470408) and the Shanxi Provincial Natural Science Foundation.

References

[1] P. Nordell, P. Lincoln, J. Am. Chem. Soc. 127 (2005) 9670.
[2] C.C. Cheng, W.C.H. Fu, K.C. Hung, P.J. Chen, W.J. Wang, Y.T. Chen, Nucl. Acid Res. 31 (2003) 2227.
[3] A.A. Mokhir, R. Kraemer, Bioconjugate Chem. 14 (2003) 877.
[4] W.C. Tse, D.L. Boger, Acc. Chem. Res. 37 (2004) 61.
[5] P. Yang, R. Ren, M.L. Guo, A.X. Song, X.L. Meng, C.X. Yuan, Q.H. Zhou, H.L. Chen, Z.H. Xiong, X.L. Gao, J. Biol. Inorg. Chem. 9 (2004) 495.
[6] A.Th. Chaviara, P.J. Cox, K.H. Repana, A.A. Pantazaki, K.T. Papazisis, A.H. Kortsaris, D.A. Kyriakidis, G.S. Nikolov, C.A. Bolos, J. Inorg. Biochem. 99 (2005) 467.
[7] A.M. Pyle, J.P. Rehmann, R. Meshoyrer, C.V. Kumar, N.J. Turro, J.K. Barton, J. Am. Chem. Soc. 111 (1989) 3051.
[8] S. Satyanarayana, J.C. Dabrowiak, J.B. Chaires, Biochemistry 31 (1992) 9319.
[9] R.J. Sundberg, R.B. Martin, Chem. Rev. 74 (1974) 471.
[10] P.E. Pjura, K. Grzeskowiak, R.E. Dickerson, J. Mol. Biol. 197 (1987) 257.
[11] M.K. Teng, N. Usman, C.A. Frederick, A.H.J. Wang, Nucl. Acid Res. 16 (1988) 2671.
[12] J. Aymami, C.M. Nunn, S. Neidle, Nucl. Acid Res. 27 (1999) 2691.
[13] J.A. Parkinson, J. Barber, K.T. Douglas, J. Rosamond, D. Sharples, Biochemistry 29 (1990) 10181.
[14] A. Fede, A. Labhardt, W. Bannwarth, W. Leupin, Biochemistry 30 (1991) 11377.
[15] A. Fede, M. Billeter, W. Leupin, K. Wüthrich, Structure 1 (1993) 177.
[16] D. Wahnon, R.C. Hynes, J. Chin, J. Chem. Soc.; Chem. Commun. (1994) 1441.
[17] L.M.T. Schnaith, R.S. Hanson, L. Que Jr., Proc. Natl. Acad. Sci. USA 91 (1994) 569.
[18] V.G. Vaidyanathan, B.U. Nair, J. Inorg. Biochem. 91 (2002) 405.
[19] C.L. Liu, S.W. Yu, D.F. Li, Z.R. Liao, X.H. Sun, H.B. Xu, Inorg. Chem. 41 (2002) 913.
[20] S.M. Wang, P.J. Huang, H. Chang, C. Cheng, S. Wang, N.C. Li, Inorg. Chim. Acta 182 (1991) 109.
[21] Y. Nakao, M. Oonishi, T. Uzu, H. Kashihara, S. Suzuki, M. Sakai, Y. Fukuda, Bull. Chem. Soc. Jap. 67 (1994) 2586.
[22] G.M. Sheldrick, SAINT v4 Software Reference Manual, Siemens Analytical X-ray Systems, Madison,WI, 1996.
[23] G.M. Sheldrick, SADABS, Program for Empirical Absorption Correction of Area Detector Data, University of Göttingen, Germany, 1996.
[24] G.M. Sheldrick, Program for the Solution of Crystal Structure, University of Göttingen, Germany, 1997.
[25] G.M. Sheldrick, Program for the Refinement of Crystal Structure, University of Göttingen, Germany, 1997.
[26] A.J. Wilson, International Table for X-ray Crystallography, vol. C, Kluwer Academic Publishers, Dordrecht, The Netherlands, 1995.
[27] G.M. Sheldrick, SHELXTL/PC. Version 5.1, Bruker AXS Inc., Madison, WI, USA, 1999.
[28] M. Baldini, M. Belicchi-Ferrai, F. Bisceglie, G. Pelosi, S. Pinelli, P. Tarasconi, Inorg. Chem. 42 (2003) 2049.
[29] J. Yang, J.F. Ma, Y.C. Liu, G.L. Zheng, L. Li, J.F. Liu, J. Mol. Struct. 646 (2003) 55.
[30] Z.R. Liao, X.F. Zheng, B.S. Luo, L.R. Shen, D.F. Li, H.L. Liu, W. Zhao, Polyhedron 20 (2001) 2813.
[31] P.M. Bush, J.P. Whitehead, C.C. Pink, E.C. Gramm, J.L. Eglin, S.P. Watton, L.E. Pence, Inorg. Chem. 40 (2001) 1871.
[32] J.K. Barton, A.T. Danishefsky, J.M. Goldberg, J. Am. Chem. Soc. 106 (1984) 2172.
[33] C.E. Bostock-Smith, M.S. Soarle, Nucl. Acid Res. 27 (1999) 1619.
[34] Q. Li, P. Yang, H. Wang, M. Guo, J. Inorg. Biochem. 64 (1996) 181.
[35] J.B. Lepecq, C. Paoletti, J. Mol. Biol. 27 (1967) 87.
[36] M.L. Guo, P. Yang, B.S. Yang, Z.G. Zhang, Chin. Sci. Bull. 41 (1996) 1098.
[37] M. Balón, M.A. Muñoz, C. Carmona, P. Guardado, M. Galán, Biophys. Chem. 80 (1999) 41.